Activating FGFR3 Y367C mutation causes hearing loss and inner ear defect in a mouse model of chondrodysplasia.

Stéphanie Pannier[1], Vincent Couloigner[2], Nadia Messaddeq[3], Monique Elmaleh-Bergès[4], Arnold Munnich[1], Raymond Romand[3], Laurence Legeai-Mallet[1] *

[1]INSERM U781-Université Paris Descartes-Hôpital Necker-Enfants Malades-149 rue de Sèvres-75015, Paris-France

[2]Service Oto-Rhino-Laryngologie-Chirurgie Cervico-faciale-Hôpital-Necker-Enfants Malades-149 rue de Sèvres-75743, Paris 15-France

[3]IGBMC, 1 rue Laurent Fries-67404, Illkirch-France

[4]Service Imagerie Pédiatrique-Hôpital Robert Debré-48 Boulevard Sérurier-75935, Paris 19-France

* To whom correspondence should be addressed.

E-mail: laurence.legeai-mallet@inserm.fr

Phone: 33144494000 ext 97830

Fax: 33147348514

Keywords: Chondrodysplasias, FGFR3, hearing loss, cochlea, pillar cells.

ABSTRACT

Fibroblast growth factor receptor 3 (FGFR3) is a key regulator of skeletal development and activating mutations in FGFR3 cause skeletal dysplasias, including hypochondroplasia, achondroplasia and thanatophoric dysplasia. The introduction of the Y367C mutation corresponding to the human Y373C thanatophoric dysplasia type I (TDI) mutation into the mouse genome, resulted in dwarfism with a skeletal phenotype remarkably similar to that of human chondrodysplasia. To investigate the role of the activating FGFR3 Y367C mutation in auditory function, the middle and inner ear of the heterozygous mutant fgfr3$^{Y367C/+}$ mice were examined. The mutant fgfr3$^{Y367C/+}$ mice exhibit mild deafness with a significantly elevated ABR threshold for all frequencies tested. The inner ear defect is mainly associated with an increased number of pillar cells or modified supporting cells in the organ of Corti. Hearing loss in the fgfr3$^{Y367C/+}$ mouse model demonstrates the crucial role of FGFR3 in the development of the inner ear and provides novel insight on the biological consequences of FGFR3 mutations in chondrodysplasia.

INTRODUCTION

Fibroblast growth factors (FGFs) and their surface receptors regulate a variety of cellular processes during embryonic and postnatal development. Four fibroblast growth factor receptors (FGFRs) are known, and three of them are associated with genetic disorders in humans [1]. Among them, FGFR3 has been recognized as a critical regulator of endochondral bone growth. Mutations in the coding sequence of the FGFR3 gene have been shown to cause achondroplasia (ACH), the most common form of dwarfism [2], hypochondroplasia (HCH), a milder phenotype [3] and thanatophoric dysplasia (TD), the most severe form of dwarfism [4, 5]. All FGFR3 mutations examined so far result in a ligand-independent phosphorylation of the tyrosine kinase domain [6]. To further study the function of FGFR3 during development, several mouse models have been created with various mutations corresponding to ACH or TD phenotypes [7-12]. The different mouse models displayed varying degrees of disproportionate dwarfism with skeletal anomalies. By contrast, the mouse model lacking fgfr3 had skeletal overgrowth and a significant hearing loss found to be due to cochlear impairment. In these mice the cochlear defect consisted of a lack of differentiation and an incomplete development of pillar cells within the organ of Corti [13-16].

In vertebrates, the perception of sounds is controlled by epithelial sensory cells located in the cochlear region of the inner ear. The sensory epithelium forms the organ of Corti which mediates the auditory function in mammals and comprises distinct cell types arranged in precise rows that extend along the entire length of the cochlear spiral. The organ of Corti contains one row of inner and three rows of outer hair cells and several types of supporting cells, namely pillar

cells, Deiter's cells, Hensen's and Claudius' cells [17]. Previous studies have demonstrated that fgfr3 is required for pillar cell development and an increase in number of both outer hair cells and Deiter's cells was recently observed in the cochleae of fgfr3 knock out mice [16]. By contrast, ectopic activation of fgfr3 by the either FGF2 or FGF8 in cochlear explants induces an overexpression of pillar cells in the organ of Corti [14, 18].

To investigate the impact of a constitutive activation of FGFR3 on cochlear development, we generated a mouse model carrying the Y367C mutation corresponding to the human Y373C TDI mutation. This mutation causes a ligand-independent activation of FGFR3 in vitro [19]. Here, we show for the first time, that the heterozygous mutant mice exhibited an inner ear defect with a significantly elevated ABR threshold in addition to severe dwarfism. Histological studies of the organ of Corti revealed an increased number of cells with the appearance of pillar cells most likely derived from Deiter's cells; we called these cells "modified Deiter's cells". Hearing loss in the fgfr3$^{Y367C/+}$ mouse emphasizes the interest in addressing the role of FGFR3 in the development of the organ of Corti.

MATERIALS AND METHODS

Generation of fgfr3$^{Y367C/+}$ mice.

The mutant construction was generated by PCR amplification of mouse 129Sv/Pas genomic DNA. The Y367C mutation was introduced into exon 9 of the mouse fgfr3 gene using oligonucleotides flanking the targeted sequence. The 468bp PCR product containing the mutation was cloned upstream of a NEO cassette flanked by LoxP recombination sites (ICS vector). Two fragments of 4.1 and 2.1 kb respectively, were added as 5' and 3' homology arms. An Fse I

restriction site was added in intron 8 for cloning purposes (-175 from exon 9) (Fig. 1A). The construct was linearized by digestion of the polylinker upstream of the 5' homology arm and electroporated in 129Sv/Pas mouse ES cells (ICS cell line). Genomic DNA from ES cell clones was digested with restriction enzymes and subjected to Southern blot analysis with either a 3' external probe or a NEO probe (Fig. 1B). The presence of the mutation in the recombinant clones was confirmed by sequencing using oligonucleotides to the NEO cassette. The 129Sv/Pas mice exhibiting germ-line transmission of the Y367C mutation were crossed with CMV-Cre mice (C57BL/6j) [20] in order to delete the NEO gene. Genotypes of the resulting offspring were determined by PCR analysis using primers 1(5'GATACCAGGTTTTGAGCTCCCTGTCC-3') and 2(5'TCAAGCCTATGAGGCAAG GTGTGG-3'). All animal studies were conducted according to an Animal study protocol approved by the animal Care and Use Committee.

Radiographs, microradiographs and scanners.

Animals were studied at birth (P0) and at five time points (P7, P14, P21, P28 and P35). All animals were euthanized by asphyxiation in CO_2. The skeletons were visualised on Kodak oncology films using a Cabinet X-ray System (Faxitron series-Hewlett Packard) (15 sec, 35 KV and 3 mA). The heads were visualised on high Resolution Film SO-343 (Kodak Professional, Paris, France) using a microfocal X-ray generator (Tubix, Paris, France) at a focal distance of 56 cm for 20 min (power setting 12 mA and 15 KV). Temporal bones were analysed using a micro-CT scanner (Skycan 1076: Skycan, Antwerp, Belgium). The X-ray source was set at 55 kV and 179 μA, with a 0.5 mm aluminium filter and a pixel size at 17.60 μm.

Bone and cartilage stain.

After removing skin, muscles and other soft tissues, the bones and heads were fixed in 95% ethanol and then stained with Alizarin Red and Alcian Blue, cleared by KOH treatment, and stored in glycerol according to standard protocols [21]. After several weeks, the heads were dissected and the three ossicles (malleus, incus and stapes) were isolated from the middle ear.

General testing procedure for auditory brainstem responses (ABRs).

Animals from a mixed background (C57BL/6j/129Sv/Pas) from 6 different litters were tested. Eight $fgfr3^{Y367C/+}$ and wild type (WT) mice were tested, at a mean age of 4 weeks (3-5 weeks). Each $fgfr3^{Y367C/+}$ mouse was tested with its WT control from the same litter. All recording sessions and data analysis were performed as described by Ouagazzal et al [22]. All experimental procedures were carried out according to European Union guidelines and were approved by the local Ethical Committee (CREMEAS).

Immunohistological analyses.

Isolated cochleae were fixed in 4% paraformaldehyde, decalcified in 0.5 M EDTA and embedded in paraffin. Sections (5 μm) were cut and stained with hematoxylin-eosin. For immunofluorescence, sections were blocked in PBST (PBS, 5% normal sheep serum, 0.1% Tween) and incubated with primary antibodies overnight at 4℃. After washing, sections were incubated with a fluorescence labelled secondary antibody. The primary antibody, an anti p75 nerve growth factor ($p75^{NGFR}$) polyclonal antibody, was purchased from Chemicon and used at a

dilution of 1/200. The labelled secondary antibody, Alexa fluor 568 goat anti rabbit antibody was purchased from Molecular Probes and used at a dilution of 1/250. Alexa fluor 488 Phalloidin (Molecular Probes) was used at a dilution of 1/50. Slides were mounted using Vectashield mounting medium with DAPI (Vector). An Olympus PD70-IX2-UCB microscope was used for reflected light fluorescence and transmitted light examination.

Histological and ultrastructural analyses.

After physiological testing, animals were decapitated and the inner ears were removed and fixed by immersion in 2.5% paraformaldehyde and 2.5% glutaraldehyde in cacodylate buffer (0.1 M, pH 7.2) overnight at 4℃. The inner ears were decalcified in 10% EDTA, dehydrated and then washed in cacodylate buffer for a further 30 min followed by post-fixation with 1% osmium tetroxide in 0.1 M cacodylate buffer for 1 h at room temperature. The specimens were dehydrated through graded alcohol series and embedded in Epon 812. Semi-thin serial sections were cut at 2.5 µm (Leica ultracut UCT), stained with Toluidine Blue and observed under a light microscope (Leitz). Transmission electron microscopy observation was performed with a Morgagni microscope (FEI) and pictures were processed with the Adobe Photoshop (version 7) software.

RESULTS

Severe dwarfism in heterozygous fgfr3$^{Y367C/+}$ mice.

To study the effect of FGFR3 mutations on the development of the skeletal and auditory system, we introduced the Y367C mutation corresponding to the human TDI mutation into the mouse genome (Fig. 1A). Germline transmission was

confirmed in targeted ES cells (Fig. 1B). The fgfr3$^{neoY367C/+}$ mice were crossed with CMV-CRE mice to excise the NEO sequence from the germline. The fgfr3$^{Y367C/+}$ mice were obtained with an expected Mendelian segregation. At P0, fgfr3$^{Y367C/+}$ mice exhibited skeletal dysplasia. The phenotype became progressively more pronounced as the mice got older and the fgfr3$^{Y367C/+}$ mice died 6-8 weeks after birth. The dwarf mice exhibited a reduced length of long bone especially femur and tail bones, a narrow trunk, short ribs and macrocephaly (Fig. 1C). Several fgfr3$^{Y367C/+}$ mice presented bowed tibia, fibula, ulna and radius. Histological examination of epiphyseal growth plates in fgfr3$^{Y367C/+}$ mice showed that the growth plate was disorganized, the chondrocyte columns were markedly shortened and hypertrophic chondrocytes were reduced in number and size (data not shown). All these observations showed that activation of fgfr3 by the Y367C mutation resulted in skeletal dysplasia in mice.

Auditory brainstem responses (ABRs) of fgfr3$^{Y367C/+}$ mice.

The auditory thresholds of eight fgfr3$^{Y367C/+}$ and wild type (WT) mice was assessed at a mean age of 4 weeks using ABRs. All WT mice exhibited normal ABR waveforms and thresholds, although threshold variability was high as shown by the standard error of the mean (SEM) values ascribed to the age at testing. The fgfr3$^{Y367C/+}$ mice displayed a significantly higher ABR threshold for frequencies between 3 to 50 KHz (two-way ANOVA), [$F(1.6)=235.8$, $p<0.0001$], with a maximum of 50 dB for the medium range frequencies, and around 30 dB for lower and higher frequencies indicating a mild hearing loss (Fig. 2).

Imaging analysis.

To investigate the bases of auditory defects in fgfr3$^{Y367C/+}$ mice, we examined the skull, the middle ear and the inner ear. The skull of fgfr3$^{Y367C/+}$ mice was markedly reduced in size along the anteroposterior axis whereas the left-right and dorsal-ventral axes were only slightly increased compared to WT mice. Radiographs of fgfr3$^{Y367C/+}$ mice showed a dome-shaped skull, with a shortened skull base, a hypoplastic midface, a prognathic mandible and an abnormal orientation of the temporal bone (Fig. 3A). The fgfr3$^{Y367C/+}$ and WT mice were analysed using temporal bone high-resolution computed tomography (HRCT). On axial views, the petrous part of the temporal bone of the fgfr3$^{Y367C/+}$ mice appeared similar to WT mice during postnatal development. The computed tomography (CT) scanners showed normal cochlea, vestibule and internal acoustic meatus (Fig. 3B). There was no obvious change in size or shape of the ossicles, nor abnormality of the incudomallear joint, incudostapedial joint, or stapes and oval window in fgfr3$^{Y367C/+}$ mice (data not shown). The region of the temporal bone corresponding to the human mastoid was poorly developed with low pneumatization in all the fgfr3$^{Y367C/+}$ mice. Finally, the foramen magnum was displaced anteriorly as a result of the shortened skull base. Conventional two-dimensional (2D) imaging was used to study ossicles and inner ear structures of the temporal bone. To better study the temporal bone and their intricate interrelationships, we used CT with three-dimensional (3D) volume rendering (VRT). Oblique or lateral 3D images showed similar results in fgfr3$^{Y367C/+}$ mice and WT mice during the postnatal period (P0-P42). The cochlea had a snail shell shape, the three canals of the cochlea winding around a central axis just over 2 1/2 times (Fig. 3C). The vestibular organs continued anteriorly with the cochlea and posteriorly with the semicircular canals. The semicircular canals formed nearly two-thirds of a circle and were enlarged

anteriorly to form the ampulla. The bony labyrinth was normal in WT and fgfr3$^{Y367C/+}$ mice (Fig. 3C).

To evaluate endochondral ossification, the three ossicles were stained with alizarin red and alcian blue. The malleus, which is the largest of the ossicles, lies anterolateral to the incus and stapes. A facet on the posterior surface of the head of the malleus articulates with the body of the incus. The anatomy of the ossicular chain in the fgfr3$^{Y367C/+}$ mice was normal. However, at P0, there was a severe ossification delay in the cochlea of fgfr3$^{Y367C/+}$ mice compared to WT mice (Fig. 3D). At P7, we observed that the orbicular apophysis of the malleus was still cartilaginous in fgfr3$^{Y367C/+}$ mice whereas it was ossified in WT mice. A similar delay was observed in the incus and the stapes (Fig. 3D). At P14, ossification of ossicles was complete in WT mice and slightly delayed in fgfr3$^{Y367C/+}$ mice. These data are consistent with the results found in long bones of fgfr3$^{Y367C/+}$ mice, where a severe ossification delay was observed at P0, P7 and P14 (data not shown).

Immunohistological studies in the cochlea.

We studied the cytoarchitecture of the organ of Corti from the first turn of the cochlear canal. At P0 and P7, WT and fgfr3$^{Y367C/+}$ mice presented a single row of inner hair cells (Fig. 4A and 4D). In addition, three or four rows of outer hair cells and Deiter's cells were almost consistently observed in WT and fgfr3$^{Y367C/+}$ mice (Fig. 4A and 4D). At P0 and P7, no gross abnormalities were observed in the basilar and tectorial membranes and the same number of pillar and Deiter's cells was stained by p75^{NGFR}, a specific marker of supporting cells in both WT and fgfr3$^{Y367C/+}$ mice (Fig. 4B and 4E). At P14, the tunnel of Corti was well formed by the pillar cells in the WT mice (Fig. 4F and 4G). By contrast, the fgfr3$^{Y367C/+}$ mice

displayed two ectopic pillars close to the first two outer hair cells in addition to the two normal pillar cells. We called these pillars “modified Deiter’s cells” because no Deiter’s cells were present at the usual place where these supporting cells are expected to be. The presence of “modified Deiter’s cells” created a larger space between outer hair cells. Usually, the same number of outer hair cells was present in WT and fgfr3$^{Y367C/+}$ mice (Fig. 4F and 4G).

Histological and ultrastructural analyses of the cochlea.

Light microscopy of the inner cochlear canals from WT and fgfr3$^{Y367C/+}$ mice of the same litter at the age of 4 weeks showed clear differences at the level of the basal cochlea up to the first turn. In a normal cochlea, Deiter’s cells support the outer hair cells at their basal poles and a lateral phalanx from the Deiter’s cell projects upward. The nucleus of Deiter’s cell is located in the upper region of the cell body, while the nucleus of the outer hair cells is in the basal region of the cell body. The most obvious differences were observed at the level of the outer hair cells and Deiter’s cells. The outer hair cells look shorter and irregularly shaped. The space between the outer hair cells (called Nuel’s space) was broader and the tunnel of Corti presented a smaller opening in fgfr3$^{Y367C/+}$ mice (compare Fig. 5A and 5D-E). The two first rows of fgfr3$^{Y367C/+}$ mice outer hair cells are not supported at their basal poles by Deiter’s cell but replaced by a pillar-like structure called “modified Deiter’s cells”. This structure directly connected the basilar membrane to the top of the organ of Corti at the level of the cuticular plate of the outer hair cells (Fig. 5A and 5D-E). Some cellular characteristics of the “modified Deiter’s cells” were reminiscent of pillar cells, such as the number of microtubules, although a greater number of microtubules were fasciculated into large bundles (Fig. 5F and 5G). In

addition, the nucleus occupied a basal position just above the basilar membrane. Other features tended to correspond to Deiter's cell characteristics such as 1) the large amount of cytoplasm on either side of the pillar-like structure (Fig. 5F and 5J), and 2) outer spiral fibers running in an invagination along the lateral cytoplasm (Fig. 5C and 5J). On the contrary, the third outer hair cells is supported by a normal Deiter's cell. As in WT mice, several afferent and efferent synaptic contacts were present in the fgfr3$^{Y367C/+}$ mice (Fig. 5B and 5I). Ultrastructural analyses of outer hair cells in the apical region showed a regular cuticular plate topped with a bundle of stereocilia (Fig. 5H). These differences were usually restricted to the basal and first turn of the cochlea and progressively disappeared in the upper regions of the cochlea.

DISCUSSION

Fibroblast growth factor receptor 3 plays an important role in the normal development of the skeleton [23] and mutations in the gene are responsible for ACH, as well as other related conditions such as TD and HCH [2-4]. Several mouse models exist in which mutations in FGFR3 resulted in skeletal conditions that mimic the human diseases [7-12, 24]. Here, we report a novel model of skeletal dysplasia corresponding to the human Y373C TD mutation, generated by introducing a Y367C point mutation into the mouse fgfr3 gene. The analysis of the long bones of fgfr3$^{Y367C/+}$ mice indicated that the growth plate was disorganized with a reduced size of the hypertrophic and proliferative zone. The fgfr3$^{Y367C/+}$ mice displayed a narrow trunk, short limbs, a shortened skull base, a large head with shortened nasal bone and prognathic mandible. All of these changes result from the disruption of endochondral ossification in the long bone and at the base of the

skull. Accordingly, we observed an abnormal orientation of the temporal bone and a delay in ossicular chain and cochlear ossification in mutant mice.

This study addresses the role of mutations in the FGFR3 gene on mild hearing loss and our data show a significantly elevated ABR threshold for all frequencies tested ($p<0.0001$) in $fgfr3^{Y367C/+}$ mice. The architecture of the organ of Corti was modified whereby the Deiter's cells adopted a phenotype intermediate between pillar cells and Deiter's cells and we therefore called these cells "modified Deiter's cells". It is interesting to note that despite the disorganization of the organ of Corti in the $fgfr3^{Y367C/+}$ mice, anatomical changes were restricted to a lateral region to the tunnel of Corti at the level of the outer hair cell region. The normal appearance of the inner hair cells and the tunnel of Corti may explain why the cochlea was still functioning [25].

Our results suggest that fgfr3 is important in the differentiation of progenitor cells into pillar cells and Deiter's cells during cochlear development and several studies support this hypothesis. Ectopic activation of fgfr3 by FGF8 or FGF2 leads to the appearance of an extra row of pillar cells in cochlear explants [14, 18]. In addition, deletion of the sprouty2 gene, a negative feedback regulator of FGFRs, causes a cochlear phenotype similar to that of the $fgfr3^{Y367C/+}$ mice. The sprouty2 knockout mice show extra pillar cells with a similar morphology to the "modified Deiter's cells" observed in the $fgfr3^{Y367C/+}$ mice [26]. Conversely, in a mouse model lacking fgfr3 opposite results were observed, namely a failure of pillar cell development and severe auditory impairment [13, 15, 16]. During the antenatal period, fgfr3 gene is initially expressed in a population of cells located at the cochlear prosensory domain, whereas at birth its expression is mainly restricted to the pillar cells and Deiter's cells [14-16, 18, 27]. The constitutive activation of fgfr3 may be

implicated in specifying the fate of progenitor cells, or induce their differentiation into pillar cells and/or Deiter's cells.

Contrary to some previous studies [18, 26], the fgfr3$^{Y367C/+}$ mice did not show any difference in the outer hair cells in the first turn of the cochlea. We hypothesize that fgfr3 may not directly be required for outer hair cell differentiation. It possible that fgfr3 plays an indirect role in regulating the normal differentiation of outer hair cells by preventing a normal development of specific proteins such as Prestin or BMPs important for the outer hair cell function [16]. Further studies of the cytoarchitecture of the organ of Corti in fgfr3$^{Y367C/+}$ mice will determine the exact consequences of FGF signaling during development.

In conclusion, the presence of extra pillar cells or "modified Deiter's cells" in the organ of Corti in the fgfr3$^{Y367C/+}$ mice is likely to be responsible for the observed hearing deficit. In human, conductive and sensorineural hearing loss have been reported in achondroplasia patients [28-30], with acute otitis media and otitis media with effusion as the most common causes of conductive hearing loss. At present no data are available to explain the sensorineural hearing loss in achondroplasia. The hearing loss observed in the mouse fgfr3$^{Y367C/+}$ model suggests that similar inner ear anatomical anomalies could be present in human chondrodysplasia with activating FGFR3 mutations. This study provides a novel insight into the biological consequences of FGFR3 mutations, and prompts the need to pay attention to sensorineural hearing loss in chondrodysplasia.

Acknowledgements

This research was supported by EUROGROW and GIS-Maladies Rares. AP-HP/CANAM was awarded to SP. We thank Gérard Pivert, Chantal Exculpavit and

Catherine Benoist-Lasselin for technical support, Eric Legall for the art work, Dr Manousous Koutsourakis (Institut clinique de la souris-Illkirch) for fgfr3 constructions, Dr Frederic Lezot (UMRS 872-Laboratoire de Biologie Orofaciale et pathologie-Paris) and Luc Magnier (Animage-Lyon) for imaging microradiographs and three-dimensional (3D) CT.

REFERENCES

[1] D.M. Ornitz, J. Xu, J.S. Colvin, D.G. McEwen, C.A. MacArthur, F. Coulier, G. Gao, M. Goldfarb. Receptor specificity of the fibroblast growth factor family. J. Biol. Chem. 271 (1996) 15292-15297.

[2] F. Rousseau, J. Bonaventure, L. Legeai-Mallet, A. Pelet, J.M. Rozet, P. Maroteaux, M. Le Merrer, A. Munnich. Mutations in the gene encoding fibroblast growth factor receptor-3 in achondroplasia. Nature 371 (1994) 252-254.

[3] G.A. Bellus, I. McIntosh, E.A. Smith, A.S. Aylsworth, I. Kaitila, W.A. Horton, G.A. Greenhaw, J.T. Hecht, C.A. Francomano. A recurrent mutation in the tyrosine kinase domain of fibroblast growth factor receptor 3 causes hypochondroplasia. Nat. Genet. 10 (1995) 357-359.

[4] F. Rousseau, P. Saugier, M. Le Merrer, A. Munnich, A.L. Delezoide, P. Maroteaux, J. Bonaventure, F. Narcy, M. Sanak. Stop codon FGFR3 mutations in thanatophoric dwarfism type 1. Nat. Genet. 10 (1995) 11-12.

[5] F. Rousseau, V. el Ghouzzi, A.L. Delezoide, L. Legeai-Mallet, M. Le Merrer, A. Munnich, J. Bonaventure. Missense FGFR3 mutations create cysteine residues in thanatophoric dwarfism type I (TD1). Hum. Mol. Genet. 5 (1996) 509-512.

[6] M.C. Naski, Q. Wang, J. Xu, D.M. Ornitz. Graded activation of fibroblast growth factor receptor 3 by mutations causing achondroplasia and thanatophoric dysplasia. Nat. Genet. 13 (1996) 233-237.

[7] M.C. Naski, J.S. Colvin, J.D. Coffin, D.M. Ornitz. Repression of hedgehog signaling and BMP4 expression in growth plate cartilage by fibroblast growth factor receptor 3. Development 125 (1998) 4977-4988.

[8] L. Chen, R. Adar, X. Yang, E.O. Monsonego, C. Li, P.V. Hauschka, A. Yayon, C.X. Deng. Gly369Cys mutation in mouse FGFR3 causes achondroplasia by affecting both chondrogenesis and osteogenesis. J. Clin. Invest. 104 (1999) 1517-1525.

[9] Y. Wang, M.K. Spatz, K. Kannan, H. Hayk, A. Avivi, M. Gorivodsky, M. Pines, A. Yayon, P. Lonai, D. Givol. A mouse model for achondroplasia produced by targeting fibroblast growth factor receptor 3. Proc. Natl. Acad. Sci. U. S. A. 96 (1999) 4455-4460.

[10] T. Iwata, L. Chen, C. Li, D.A. Ovchinnikov, R.R. Behringer, C.A. Francomano, C.X. Deng. A neonatal lethal mutation in FGFR3 uncouples proliferation and differentiation of growth plate chondrocytes in embryos. Hum. Mol. Genet. 9 (2000) 1603-1613.

[11] T. Iwata, C.L. Li, C.X. Deng, C.A. Francomano. Highly activated Fgfr3 with the K644M mutation causes prolonged survival in severe dwarf mice. Hum. Mol. Genet. 10 (2001) 1255-1264.

[12] C. Li, L. Chen, T. Iwata, M. Kitagawa, X.Y. Fu, C.X. Deng. A Lys644Glu substitution in fibroblast growth factor receptor 3 (FGFR3) causes dwarfism in mice by activation of STATs and ink4 cell cycle inhibitors. Hum. Mol. Genet. 8 (1999) 35-44.

[13] J.S. Colvin, B.A. Bohne, G.W. Harding, D.G. McEwen, D.M. Ornitz. Skeletal overgrowth and deafness in mice lacking fibroblast growth factor receptor 3. Nat. Genet. 12 (1996) 390-397.

[14] K.L. Mueller, B.E. Jacques, M.W. Kelley. Fibroblast growth factor signaling regulates pillar cell development in the organ of corti. J. Neurosci. 22 (2002) 9368-9377.

[15] T. Hayashi, D. Cunningham, O. Bermingham-McDonogh. Loss of Fgfr3 leads to excess hair cell development in the mouse organ of Corti. Dev. Dyn. 236 (2007) 525-533.

[16] C. Puligilla, F. Feng, K. Ishikawa, S. Bertuzzi, A. Dabdoub, A.J. Griffith, B. Fritzsch, M.W. Kelley. Disruption of fibroblast growth factor receptor 3 signaling results in defects in cellular differentiation, neuronal patterning, and hearing impairment. Dev. Dyn. 236 (2007) 1905-1917.

[17] M.W. Kelley. Regulation of cell fate in the sensory epithelia of the inner ear. Nat. Rev. Neurosci. 7 (2006) 837-849.

[18] B.E. Jacques, M.E. Montcouquiol, E.M. Layman, M. Lewandoski, M.W. Kelley. Fgf8 induces pillar cell fate and regulates cellular patterning in the mammalian cochlea. Development 134 (2007) 3021-3029.

[19] L. Gibbs, L. Legeai-Mallet. FGFR3 intracellular mutations induce tyrosine phosphorylation in the Golgi and defective glycosylation. Biochim. Biophys. Acta 1773 (2007) 502-512.

[20] D. Metzger, J. Clifford, H. Chiba, P. Chambon. Conditional site-specific recombination in mammalian cells using a ligand-dependent chimeric Cre recombinase. Proc. Natl. Acad. Sci. U. S. A. 92 (1995) 6991-6995.

[21] C. Deng, A. Wynshaw-Boris, F. Zhou, A. Kuo, P. Leder. Fibroblast growth factor receptor 3 is a negative regulator of bone growth. Cell 84 (1996) 911-921.

[22] A.M. Ouagazzal, D. Reiss, R. Romand R. Effects of age-related hearing loss on startle reflex and prepulse inhibition in mice on pure and mixed C57BL and 129 genetic background. Behav. Brain. Res. 172 (2006) 307-315.

[23] B.R. Olsen, A.M. Reginato, W. Wang. Bone development. Annu. Rev. Cell Dev. Biol. 16 (2000) 191-220.

[24] L. Chen, C. Li, W. Qiao, X. Xu, C. Deng. A Ser(365)-->Cys mutation of fibroblast growth factor receptor 3 in mouse downregulates Ihh/PTHrP signals and causes severe achondroplasia. Hum. Mol. Genet. 10 (2001) 457-465.

[25] P. Dallos. The active cochlea. J. Neurosci. 12 (1992) 4575-4585.

[26] K. Shim, G. Minowada, D.E. Coling, G.R. Martin. Sprouty2, a mouse deafness gene, regulates cell fate decisions in the auditory sensory epithelium by antagonizing FGF signaling. Dev. Cell 8 (2005) 553-564.

[27] K. Peters, D. Ornitz, S. Werner, L. Williams. Unique expression pattern of the FGF receptor 3 gene during mouse organogenesis. Dev. Biol. 155 (1993) 423-430.

[28] M. Shohat, E. Flaum, S.R. Cobb, R. Lachman, C. Rubin, C. Ash, D.L. Rimoin. Hearing loss and temporal bone structure in achondroplasia. Am. J. Med. Genet. 45 (1993) 548-551.

[29] R.F. Gorlin, J.J. Pinborg, M.M. Cohen. Syndromes of the head and neck. 2th edn. Oxford University Press. New York, 1976, pp. 171-174.

[30] W.O. Collins, S.S. Choi. Otolaryngologic manifestations of achondroplasia. Arch. Otolaryngol. Head Neck Surg. 133 (2007) 237-244.

Figure legends

Figure 1: Generation of the dwarf fgfr3$^{Y367C/+}$ mouse.

(A) The point mutation Y367C in mouse exon 9 was co-transferred with the neomycin gene (NEO) flanked by LoxP sites, into intron 9 through homologous recombination in ES cells. Once germ-line transmission was established, fgfr3$^{\mathbf{neo}Y367C/+}$ mice were crossed with CMV-Cre mice to remove the NEO gene.

(B) Identification of ES cells and mice carrying the fgfr3^{Y367C} allele by Southern blot following digestion of genomic DNA with Bam HI and Hind III.

(C) Radiographs in three week-old fgfr3$^{Y367C/+}$ (right) and wild-type (WT) littermate mice (left). Note the narrow trunk, short ribs and long bones, and macrocephaly in the fgfr3$^{Y367C/+}$ mouse.

Figure 2: Auditory deficits in fgfr3$^{Y367C/+}$ mice.

Auditory Brainstem Response (ABR) thresholds from 8 fgfr3$^{Y367C/+}$ mice and 8 WT mice at a mean age of 4 weeks (3-5 weeks). The fgfr3$^{Y367C/+}$ displayed a mild deafness with an elevated ABR threshold for frequencies between 3 to 50 KHz. Vertical bars indicate S.E.M.

Figure 3: Analysis of the middle and inner ear.

(A) Microradiograph of the skull of the fgfr3$^{Y367C/+}$ mouse at P14 showing a dome-shaped skull, a shortened cranial base, a hypoplastic midface, a prognathic mandible (Md), an abnormal orientation of the semi circular canals (SCC), cochlea (Co) and foramen magnum (Fm) in the temporal bone.

(B) High resolution computed tomography (HRCT) scanning reveals a normal cochlea (Co), vestibule (Ve) and internal acoustic meatus (IAM) in both WT and

fgfr3$^{Y367C/+}$ mice at P21. The temporal bone (TB) is poorly developed in fgfr3$^{Y367C/+}$ mice.

(C) Three dimensional (3D) images of the bony labyrinth which consist of the vestibule (Ve), the semi circular canals (SCC) and the cochlea (Co) with the oval window (OW) and round window (RW) in three week-old fgfr3$^{Y367C/+}$ and WT mice.

(D) Staining of the bony capsule of the inner ear and the ossicles from the middle ear shows delayed ossification in the bony capsule of the fgfr3$^{Y367C/+}$ mice at P0. Ossification of the cochlea (Co) was delayed in fgfr3$^{Y367C/+}$ mice. At P7, the orbicular apophysis of the malleus (Ma) (arrow), the incus (In) and the stapes (St) were still cartilaginous in the fgfr3$^{Y367C/+}$ mice. One week later, at P14, the ossicles were slightly delayed in fgfr3$^{Y367C/+}$ mice and totally ossified in WT.

Figure 4: Modifications of the organ of Corti in fgfr3$^{Y367C/+}$ mice

(A and B) Cross sections of the first turn of the cochlear canal through the organ of Corti (OC) at P0 were stained with phalloidin (green), DAPI (blue) and p75^{NGFR} (red). The mutant and WT mice presented a normal number of cells in the organ of Corti: one inner hair cell (IHC), two pillar cells, three outer hair cells (OHC) and three Deiter's cells (DC). (A: phase contrast, B: immunofluorescence).

(C) Schematic drawing of cross-sectional views of the organ of Corti in the WT and fgfr3$^{Y367C/+}$ mice at P0. The organ of Corti is composed of an outer pillar (OP), an inner pillar (IP) (orange), Deiter's cells (DC) (red), inner hair cells (IHC) and outer hair cells (OHC) (green).

(D and E) Cross sections through the organ of Corti of fgfr3$^{Y367C/+}$ mice at P7 showing the same number of cells as seen at birth in the WT mice, except for the

presence of four outer hair cells (OHC) in this case. $P75^{NGFR}$ labels pillar cells (PC) and Deiter's cells (DC).

(F) Cross-sections through the organ of Corti at P14, stained for phalloidin and counterstained with DAPI. Two modified Deiter's cells (MDC) were present in the $fgfr3^{Y367C/+}$ mice and large spaces are visible between rows of outer hair cells (OHC) (asterisks).

(G) Schematic drawing of the mature organ of Corti in WT and $fgfr3^{Y367C/+}$ mice at P14. Note the presence of two modified Deiter's cells (MDC) (red) and large spaces (asterisks) between outer hair cells (OHC) in the mutant mice. Magnification X63 (A,B,D,E,F).

Figure 5: Light and transmission electron micrographs (TEM) of 4 week old $fgfr3^{Y367C/+}$ and WT cochleae

(A) Light micrograph of the first turn of the cochlear canal of WT mouse. The cochlear canal consists of two types of sensory cells, one row of inner hair cells (IHC) and 3 rows of outer hair cells (OHC) separated by the tunnel of Corti (TC) with two pillar cells, the inner pillar (IP) and the outer pillar (OP). The inner and outer pillar nuclei are located on the base of the basilar membrane (BM). The large open space between the IP and the first OHC is termed Nuel's space (NS). Each outer hair cell is supported by a Deiter's cell (DC). The efferent fibers, called medial olivocochlear fibers (MOC) can be observed crossing the upper part of the tunnel of Corti.

(B) Transmission electron micrograph at the synaptic pole from an outer hair cell (OHC) of the first row showing two efferent synapses (e), both synapses and the

basal pole of the outer hair cells are surrounded by a Deiter's cell (DC) in WT mouse.

(C) Transmission electron micrograph of the first Deiter's cell (DC) showing a bundle of microtubules (mt) and outer spiral fibers (osf) running in an invagination of the lateral cytoplasm in WT mouse.

(D) Light micrograph from the first turn of the cochlear canal from a fgfr3$^{Y367C/+}$ mouse. The inner hair cell (IHC) is separated from outer hair cells (OHC) by the tunnel of Corti where the lumen appears smaller. The two first rows of outer hair cells are not supported at their basal poles by Deiter's cell (DC) but are replaced by a pillar-like structure called "modified Deiter's cells" (MDC). Upper efferent tunnel crossing fibers corresponding to medial olivocochlear fibers (MOC) are visible. Spaces (asterisks) between outer hair cells, called Nuel's space (NS), are larger.

(E) Light micrograph from the first turn of the cochlear canal of the fgfr3$^{Y367C/+}$ mouse. Note that the outer hair cells (OHC) are free-standing in the space between the "modified Deiter's cells" (MDC). The nucleus of the "modified Deiter's cells" (white arrowhead) is situated close to the basilar membrane (BM).

(F) Transmission electron micrographs of the boxed area a from Figure E. The first MDC presents a large concentration of well-oriented microtubules (mt) with reduced cytoplasmic area (ca).

(G) The outer pillar (OP) is mainly composed of microtubules without much cytoplasm visible in boxed area b from Figure E.

(H) Transmission electron micrograph from box c of Figure E corresponding to the first and second rows of outer hair cells (OHC) and the first "modified Deiter's cell" (MDC).

(I) Transmission electron micrograph from the boxed area of Figure H from the synaptic pole of the outer hair cells (OHC). The “modified Deiter’s cells” (MDC) are in close contact with the outer hair cells (arrow heads). An outer spiral fiber (OSF) is seen in close contact with the MDC. Two synaptic contacts are visible below the outer hair cells. a: afferent, e: efferent synapses.

(J) Transmission electron micrograph from a lateral region of the “modified Deiter’s cells” (MDC) from the first row showing several outer spiral fibers (OSF).

Scale bars : B, C, G, J and I: 1µm, F: 0.5 µm, H: 5µm.

Figure 1

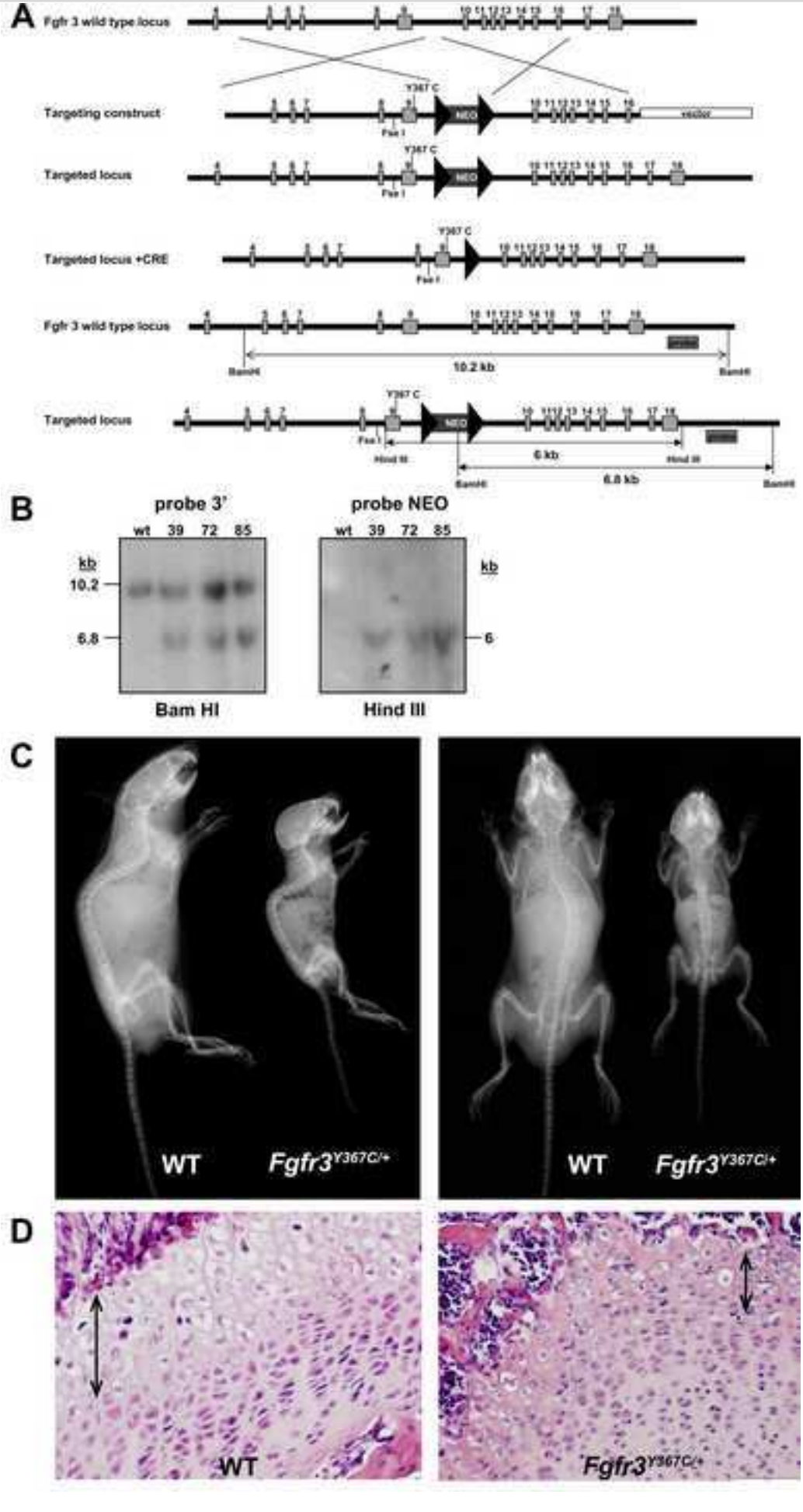

Figure 2

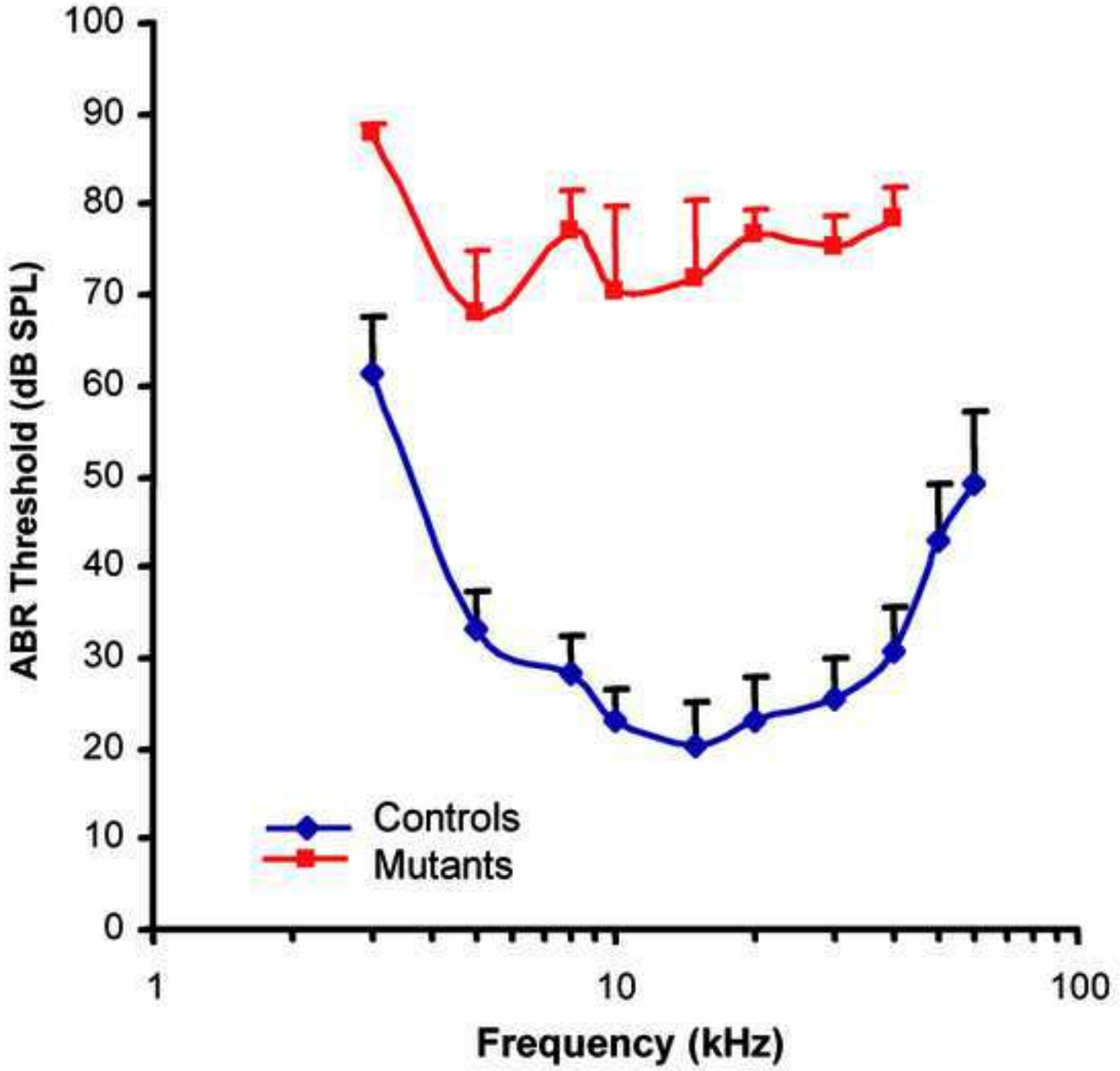

Figure 3

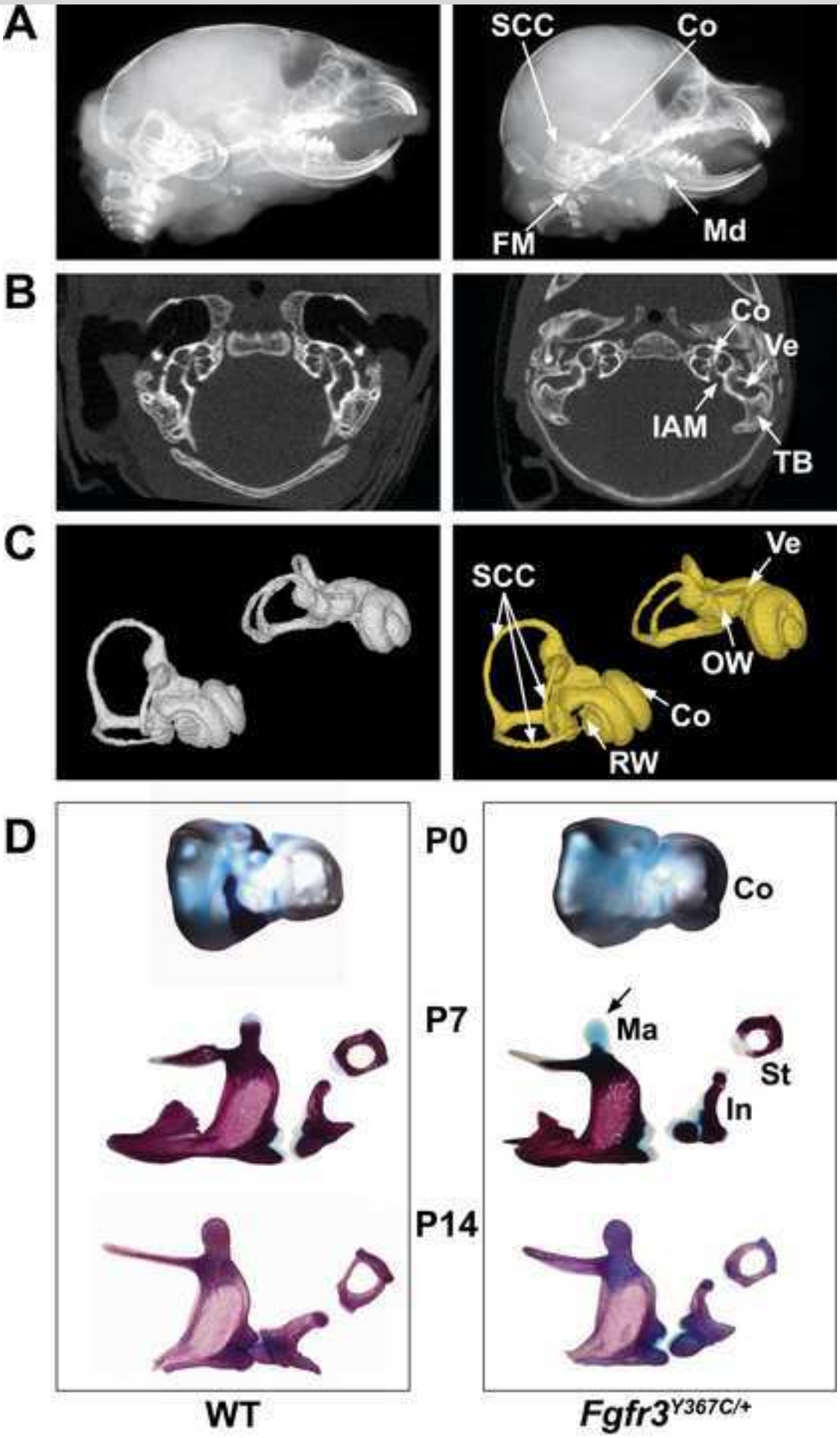

Figure 4

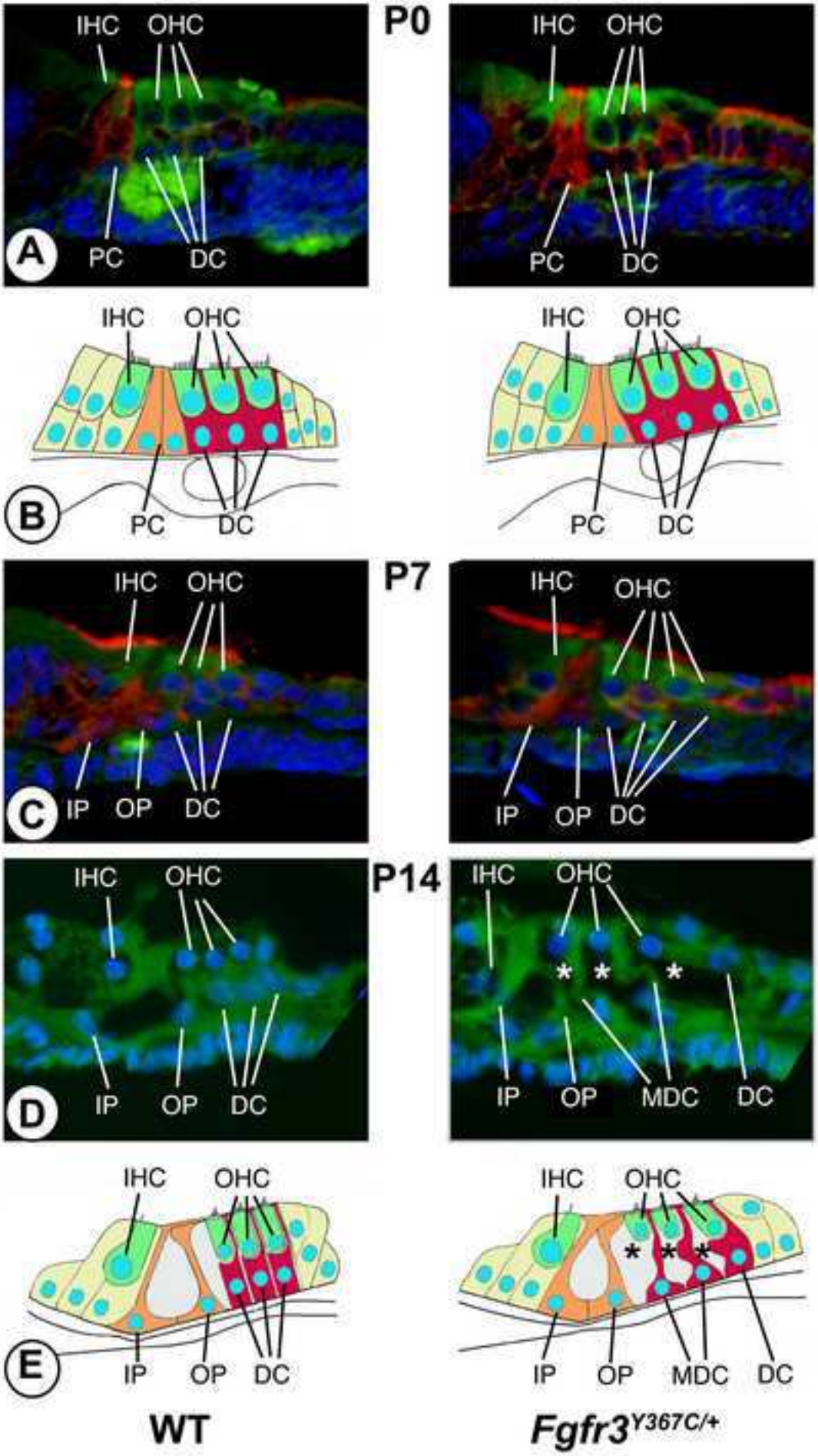

Figure 5